Antiangiogenic effects of catalpol on rat corneal neovascularization

YUN HAN[1], MEI SHEN[1], LI-YUAN TANG[2], GANG TAN[3], QI-CHEN YANG[1], LEI YE[2], LIN-HONG YE[2], NAN JIANG[2], GUI-PING GAO[2] and YI SHAO[2]

[1]Eye Institute of Xiamen University, Medical College of Xiamen University, Fujian Provincial Key Laboratory of Ophthalmology and Visual Science, Xiamen, Fujian 361102; [2]Department of Ophthalmology, The First Affiliated Hospital of Nanchang University, Nanchang, Jiangxi 330006; [3]Department of Ophthalmology, The First Affiliated Hospital of University of South China, Hengyang, Hunan 421001, P.R. China

Received April 3, 2017; Accepted September 11, 2017

DOI: 10.3892/mmr.2017.8114

Abstract. To investigate the effects of catalpol on corneal neovascularization (CNV) and associated inflammation, eye drops (5 mM catalpol or PBS) were administered four times daily to alkali-burn rat models of CNV and inflammation. Clinical evaluations of CNV and the degree of inflammation were performed on days 0, 4, 7, 10 and 14 under slit lamp microscopy. Eyes were collected on day 14 and prepared for hematoxylin and eosin, and immunofluorescence staining; corneal cell apoptosis was investigated via terminal deoxynucleotidyl transferase-mediated nick end labeling (TUNEL) staining. Protein expression levels of angiogenic and proinflammatory factors, including vascular endothelial growth factor (VEGF), pigment epithelium-derived factor (PEDF), tumor necrosis factor-α (TNF-α) and necrosis factor-κB (NF-κB) were determined by western blotting. The effects of catalpol on cell proliferation were investigated *in vitro* using human umbilical vein endothelial cells (HUVECs) and a Cell Counting kit-8 (CCK-8); alterations in migration and tube formation were investigated via HUVEC wound closure and tube formation assays. HUVEC viability and proliferative ability were inhibited in a dose-dependent manner; catalpol also decreased HUVEC cell migration and tube forming ability. Within alkali-burn rat models, decreased inflammation and CNV was associated with catalpol administration; as demonstrated with TUNEL, corneal cell apoptosis was decreased in response to catalpol. Western blot analysis revealed reduced protein expression levels of VEGF and TNF-α; however, PEDF and phosphorylated-NF-κB p65 were increased due to catalpol administration. The present study demonstrated the inhibitory effects exerted by catalpol on CNV and inflammation within alkali-burned rat models. Topical application of catalpol *in vivo* was associated with reduced CNV and inflammation; therefore, catalpol may be considered an anti-inflammatory agent for the clinical treatment of CNV.

Correspondence to: Professor Yi Shao, Department of Ophthalmology, The First Affiliated Hospital of Nanchang University, 17 Yongwaizheng Street, Nanchang, Jiangxi 330006, P.R. China
E-mail: freebee99@163.com

Key words: catalpol, corneal alkali burn, neovascularization

Introduction

Corneal disease is the second leading cause of blindness worldwide, as the cornea serves an important role in the refraction of light through the eye (1). However, local factors or systemic diseases can affect corneal transparency, which leads to the formation of corneal neovascularization (CNV), causing decreased visual acuity, corneal scar, lipid deposition and induced corneal transplant rejection (2). CNV can be induced by alkali burns. Fats and proteins are dissolved within alkali burns, which cause cellular decomposition and necrosis, and consequent corneal degeneration, necrosis, ulceration, perforation and NV. It is very important to control the inflammatory reaction and the invasion of CNV in order to reduce corneal injury and complications. The clinical use of anti-inflammatory glucocorticoids can inhibit CNV but several side effects have been reported, including intraocular pressure, infection and resistance (3). Such treatment cannot be administered onto the ocular surface safely for long durations. The present study aimed to investigate the use of catalpol to treat CNV in a safe and effective manner.

Catalpol, which is a member of the iridoid glycosides family, is a chemical component isolated from the *Scrophulariaceae rehmannia* root (4). A recent study suggested that catalpol exerts protective effects against cerebral ischemia, dementia, inflammation, capillary permeability, tumor, laxation and blood glucose levels, and other pharmacological properties associated with high safety and low toxicity (5). It has been reported that catalpol can protect neurons from cytotoxic damage, reduce neuronal cell apoptosis following cerebral ischemia (6) and alleviate neuropathic pain (7). Our previous studies have demonstrated that netrin-1 suppressed corneal and retinal NV (8-10).

Numerous neuroprotective and anti-inflammatory effects exhibited by catalpol have been reported; however,

the underlying mechanism has yet to be determined. In the present study, corneal alkali-burn rat models of CNV were employed to investigate the effects of catalpol on angiogenesis and inflammation; the potential underlying anti-angiogenic mechanism was investigated *in vitro*.

Materials and methods

Reagents and cell culture. Catalpol was isolated from the traditional Chinese medicinal root, *Scrophulariaceae rehmannia*. Catalpol was purchased from Shanghai Yuanye Biotechnology Co., Ltd. (Shanghai, China). Catalpol was dissolved in PBS to generate various concentrations, 0.1, 0.5, 1, 2, 5, 10 and 20 mM; preservatives were not used in the present study. Human umbilical vein endothelial cells (HUVECs) were obtained from the Cell Line Bank of the Chinese Academy of Sciences (Shanghai, China) and cultured as previously described (11). HUVECs were used after 2-6 passages.

Cell viability assay. The Cell Counting kit-8 (CCK-8; Dojindo Molecular Technologies, Inc., Kumamoto, Japan) assay was used to quantify cell according to the manufacturer's protocol. Briefly, $5x10^3$ HUVECs/well were seeded into 96-well plates in triplicate and incubated at 37˚C for 24 h. Catalpol was applied to the EGM-2 medium (cat. no: CC-3156; Lonza Group, Ltd., Basel, Switzerland), at a dosage of 0.1, 0.5, 1, 2, 5, 10 and 20 mM for 72 h. Cell viability was determined using 10 μl CCK-8 solution (Dojindo Molecular Technologies, Inc.), according to the manufacturer's protocol. Optical density was determined with a universal microplate reader at 450 and 570 nm (BioTek Instruments, Winooski, VT, USA),

Wound closure assay. HUVEC migration was investigated as previously described (10). HUVECs ($1x10^5$/well) were seeded onto 1% gelatin-coated 24-well plates (Corning Life Sciences, Amsterdam, Netherlands). A scratch wound was made in confluent cell culture in two perpendicular directions with a sterile pipet tip (200 μl). Floating cells were washed with PBS and the remaining cells were cultured with experimental medium (with or without 5 mM catalpol) for an additional 24 h.

In vitro tube formation assay. HUVECs were serum-starved for 12 h and seeded onto growth factor-depleted Matrigel (BD Biosciences, Franklin Lakes, NJ, USA) coated 24-well plates at a density of 10,000 cells/well. Cells were incubated at 37˚C with 5 mM catalpol or PBS (control) for 6 h and fixed with 4% paraformaldehyde (PFA). Tube structures within ≥5 microscopic fields were imaged and quantified; tube length was analyzed via ImageJ software version 2X (National Institutes of Health, Bethesda, MD, USA) (7).

Alkali-burned rat cornea model. Alkali burns were applied to Sprague Dawley rats (180-220 g; 2 months old; male; n=60; Shanghai Shilaike Laboratory Animal Co., Ltd., Shanghai, China) as previously reported (8). The rats were individually housed in hanging wire cages (changed weekly) with in a room maintained at 22±2˚C, relative humidity of 30-70%, 10 changes of air per hour, and a 12-h light/dark cycle. Tap water and standard diet were supplied *ad libitum*. Briefly, 60 anesthetized rats (10% chloral hydrate, 3 ml/kg) received topical administration of a drop of 0.5% tetracaine. Alkali burns were induced by placing 3.5 mm diameter round filter paper soaked with 1 M NaOH onto the center of the corneal surface for 30 sec, followed by a rinse of 10 ml PBS.

Alkali-burned animals were randomly divided into the PBS and catalpol groups (n=30 rats/group). Topical administrations of 10 μl PBS or 5 mM catalpol were applied four times per day for 14 days; treatments were applied every 6 h (6:00 a.m., 12:00 p.m., 6:00 p.m. and 12:00 a.m.). Eyes were examined on days 1, 4, 7, 10 and 14 by slit lamp microscopy to evaluate CNV, inflammation and damage. Rats were sacrificed on postoperative day 7 or 14, and corneal samples were collected for histological examination, protein extraction or stored at -80˚C until use.

Animal experiments were carefully performed in accordance with the guidelines of the Association for Research in Vision and Ophthalmology (Rockville, MD, USA) Statement for the Use of Animals in Ophthalmic and Vision Research (9), and the present study was approved by the Experimental Animal Committee of Xiamen University (Xiamen, China; approval ID: XMUMC2015-02-1).

Slit lamp microscopy examination. Corneal epithelial alterations were determined by 0.1% fluorescein sodium staining under cobalt blue light. Images were processed with Image Pro Plus version 6.0 (Media Cybernetics, Silver Spring, MD, USA). CNV area (S) was quantified using the following formula: $S=C/12\pi \times [r^2-(r-I)^2]$; where C is time, I is the vessel radius and r is the cornea radius (8). The inflammatory index was evaluated based on various parameters as previously described, including ciliary hyperemia, peripheral and central corneal edema (12).

Histology. Eye samples were fixed in 4% PFA in PBS overnight at 4˚C, dehydrated in a series of alcohol and embedded in paraffin. Tissue samples were cut into 5 μm sections and were subsequently stained with hematoxylin and eosin examined using an Eclipse 50i clinical microscope (Nikon Corporation, Tokyo, Japan).

Immunofluorescent staining. Cryosections of 4 μm were air-dried at room temperature for 30 min and fixed in acetone for 10 min at -20°C. Then, sections were rehydrated in PBS, and incubated in 0.2% Triton X-100 for 10 min

Following three rinses with PBS for 5 min each and preincubation with 2% BSA to block nonspecific staining, samples were incubated with anti-rabbit VEGF (cat. no: ab46154; 1:200; Abcam, Cambridge, MA, USA) and anti-rabbit PEDF (cat. no: sc-25594; 1:200; Santa Cruz Biotechnology, Inc., Dallas, TX, USA) antibodies for 16 h at 4˚C. Following three washes with PBS for 15 min, samples were incubated with a FITC-conjugated secondary antibody (goat anti-rabbit IgG; cat. no. F-6005; Lot: 065k6224; 1:100, Sigma-Aldrich; Merck KGaA, Darmstadt, Germany) for 1 h. Following three additional PBS washes, the sections were counterstained with propidium iodide (1:1,000) and then counterstained with DAPI (Vector Laboratories, Inc., Burlingame, CA, USA), mounted, and photographed using the Leica upright microscope (DM2500; Leica Microsystems GmbH, Wetzlar, Germany).

For analysis of integrated optical density expression of positive immunostaining, images from immunostained (VEGF and PEDF proteins) sections were processed using image-processing software (Image Pro Plus version 6.0; Media Cybernetics, Bethesda, MD).

Western blot analysis. Corneal tissues were dissected and ground in cold radioimmunoprecipitation assay buffer with proteinase inhibitor cocktail (Merck KGaA, Darmstadt, Germany). Total protein was quantified using a bicinchoninic acid assay and 20 μg were loaded onto 10% Bis-Tris SDS-PAGE gels under reducing conditions at (80 V, 3 h, room temperature) and then transferred onto nitrocellulose membranes. The membranes were blocked with ChemiBlocker for 1 h and the blots are subsequently incubated overnight at 4˚C with primary antibodies against VEGF (cat. no. ab46154; 1:200; Abcam, Cambridge, MA, USA), PEDF (cat. no. sc-25594; 1:200; Santa Cruz Biotechnology, Inc., Dallas, TX, USA), TNF-α (cat. no. ab66579; 1:200; Abcam) and phosphorylated p-NF-κB p65 (cat. no. sc-3033S; 1:200; Santa Cruz Biotechnology, Inc.) overnight. β-actin (cat. no. A5316; 1:10,000; Sigma-Aldrich; Merck KGaA) was used as the loading control overnight at 4˚C. Subsequently, membranes were incubated with horseradish peroxidase-conjugated secondary antibodies (Goat Anti Rabbit IgG HRP Affinity, cat. no. HAF008; 1:5,000; R&D Systems, Inc., Minneapolis, MN, USA) for 1 h at 37˚C and were visualized by enhanced chemiluminescence (ECL, lot no:161203-85, Advansta Inc., Menlo Park, CA, USA). The results were visualized and recorded on film by a Chemi DOC™ XRS Imaging System (Bio-Rad Laboratories, Inc., Hercules, CA, USA).

Apoptosis detection assay. Corneal cell apoptosis was analyzed using frozen corneal sections and terminal deoxynucleotidyl transferase-mediated nick end labeling (TUNEL; DeadEndä Fluorometric TUNEL system; Promega Corporation, Madison, WI, USA) according to the manufacturer's protocol following 4% PFA fixation overnight at 4˚C. Nuclei were counterstained with DAPI and 3 fields of view per sample were mounted in H-1200 (Vector Laboratories, Inc., Burlingame, CA, USA) and observed under a confocal microscope (Fluoview FV1000; Olympus Corporation, Tokyo, Japan).

Statistical analysis. Data are presented as the mean ± standard deviation. The inflammatory index and CNV area were analyzed with one-way analysis of variance followed by a Bonferroni post hoc comparison. One-way analysis of variance followed by a post hoc Tukey test were used to analyze HUVEC viability, migration and tube formation between groups. Statistical analyses were conducted using GraphPad software version 5 and analyzed using t-test (GraphPad Software, Inc., La Jolla, CA, USA). $P<0.05$ was considered to indicate a statistically significant difference.

Results

Catalpol decreases HUVEC viability in a dosage-dependent manner. The present study performed CCK-8 assays to determine cell viability in the presence of various concentrations of catalpol (0, 0.1, 0.5, 1, 2, 5, 10 and 20 mM). Treatment with ≥0.5 mM catalpol inhibited HUVEC survival *in vitro* (Fig. 1A). In addition, in the pre-experiment, 5 mM catalpol was reported to exert an effect on the rat model *in vivo*. In the pre-experiment, 5 mM catalpol reduced CNV and inflammation in alkali-burned rats. The CNV area at day 4, 7,10 and 14 was ~37.8, 53, 68 and 65mm^2 in the control group, and was ~25.2, 32, 35 and 30 mm^2 in the catalpol-treated group. The inflammation index at day 4, 7,10 and 14 was ~0.58, 0.63, 0.59 and 0.55 in the control group, and was ~0.43, 0.35, 0.31 and 0.24 in the catalpol-treated group (data not shown). Therefore, 5 mM catalpol was chosen for subsequent experiments.

Catalpol inhibits HUVEC migration and tube formation. In order to confirm the role of catalpol in cell proliferation, the present study assessed its effects on HUVEC migration using a scratch-wound model. Wound closure was detected in the presence of absence of catalpol. In the PBS control group, wound closure was detected within ~12 h. However, wounds in the catalpol group did not heal within 12 h; 50% of the wound remained unhealed in the catalpol-treated group at 12 h. The migration rates at 12 h were 100 and 50% in the control and 5 mM catalpol-treated groups, respectively (Fig. 1B and C).

Subsequently, the effects of catalpol on HUVEC tube formation were assessed using a previously established *in vitro* tubulogenesis assay (13). The results demonstrated that 5 mM catalpol significantly inhibited HUVEC tube formation (Fig. 1D and E).

Metabolic conditions in Sprague Dawley rats. A total of 60 weight-matched Sprague Dawley rats (weight, 200-220g; age, 8-10 weeks; male) were randomly divided into two groups, which were treated with PBS (control) or catalpol. A total of 4, 7, 10 and 14 days following administration of PBS or catalpol eye drops, body weight and eyeball weight were measured (Fig. 2A). No significant difference was observed between the experimental and control groups with regards to alterations in body weight and eyeball weight (Fig. 2B and C).

Catalpol reduces CNV in alkali-burned rat corneas. Alkali burn is a well-established model used to study CNV. The present study evaluated the effects of catalpol on CNV using an alkali burn model. Few peripheral neovascularization were detected on day 1 post-alkali burn (Fig. 3A and B). The inflammatory index was slightly decreased from day 4 to day 14 in the PBS group, whereas it was markedly reduced in the catalpol-treated group. There were significant differences between the two groups on days 4, 7, 10 and 14 (Fig. 3C).

In the PBS group, angiogenesis was detected in the peripheral corneas at around day 4, and approached the central corneas on day 7; the newly formed blood vessels were detectable on day 14 (Fig. 3A and B). Conversely, corneas treated with catalpol exhibited a mild increase in newly formed blood vessels, which were maintained at low levels throughout the study period (Fig. 3A). The area of the newly formed blood vessels was much lower in the catalpol-treated group compared with in the control group on day 14 (Fig. 3A). Persistent angiogenesis was detected in the anterior region of the corneal stroma in the control group on day 14, as determined by hematoxylin and eosin staining, and clearly indicated by the red blood cells in the blood vessels. However, in the catalpol-treated group

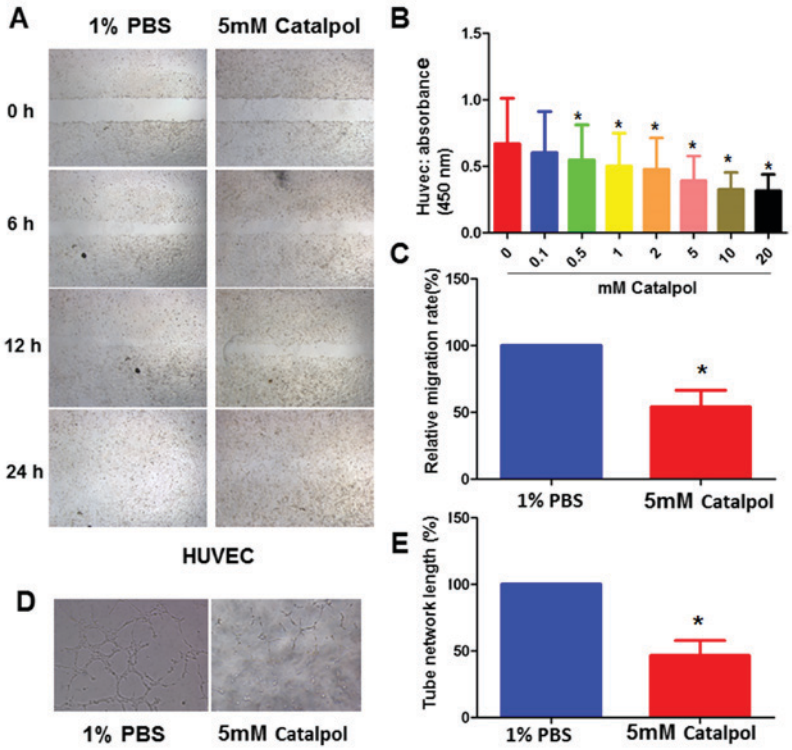

Figure 1. Effects of catalpol on HUVEC migration, viability and tube formation. (A) Cell viability was detected using the Cell Counting kit-8 assay. (B) HUVECs were cultured without serum, with or without catalpol (5 mM) and wound closure was detected. Images were captured at 0, 6, 12 and 24 h post-insert removal, magnification 10x. (C) Results are presented as wound closure percentage. (D) Tube formation was evaluated using an *in vitro* tubulogenesis assay model, magnification 20x. (E) Results were quantified 6 h following the addition of catalpol (5 mM) or PBS (control) using ImageJ. Representative images of three independent experiments are presented (n=5 wells). *P<0.05 vs. control. HUVECs, human umbilical vein endothelial cells.

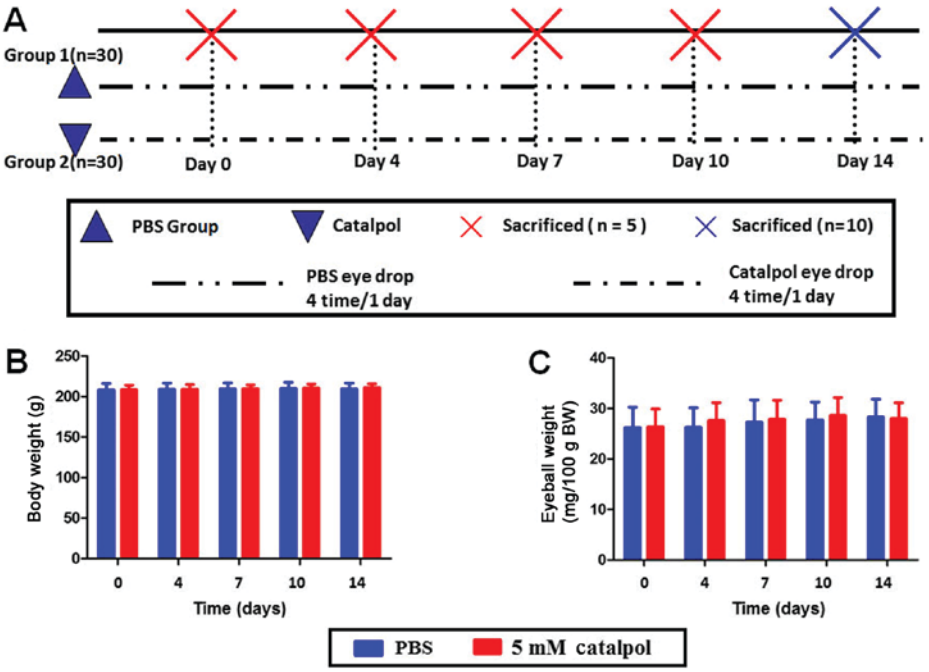

Figure 2. (A) Animal experimental design. (B) Body weight and (C) eyeball weight of Sprague Dawley rats in the experimental and control groups. There was no significant difference between the groups. There were 60 rats in total. Each group had 30 rats; 5 rats in each group were sacrificed on days 0, 4, 7 and 10 and 10 rats sacrificed on day 14.

only a few blood vessels developed in the limbus and none were detected in the peripheral or central corneas (Fig. 3A).

Catalpol reduces the alkali burn-induced apoptosis of corneal cells. Alkali burns may directly damage corneal epithelia

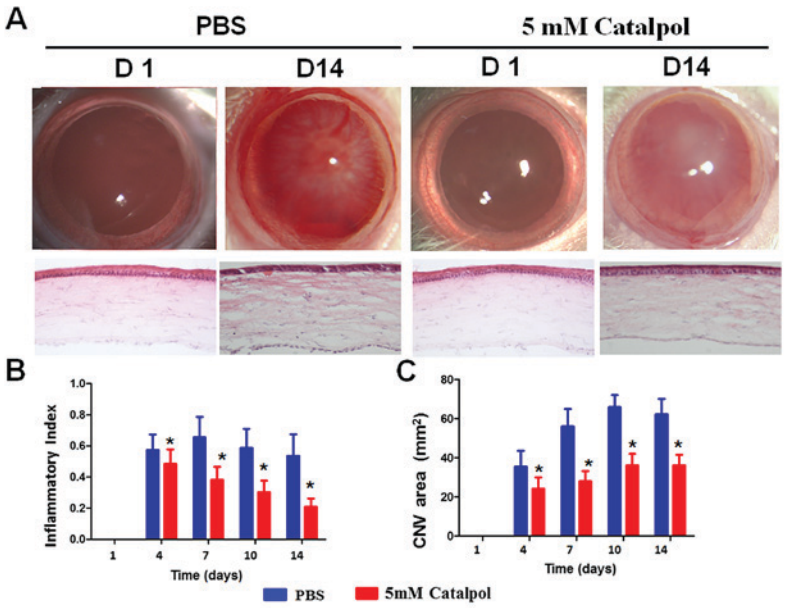

Figure 3. Catalpol reduces CNV and inflammation post-alkali burn. (A) On day 14, newly formed blood vessels approached the central part of the cornea in the control group, and corneal transparency was markedly decreased. However, only a few newly formed blood vessels in the limbus were detected in the catalpol-treated group, and the corneas remained transparent on day 14. Hematoxylin and eosin staining demonstrated that new blood vessels (white arrows) were present in the limbus and the central corneas in the control group on day 14, whereas in the catalpol-treated group, few blood vessels (white arrows) were detected in the limbus, and none were present in the peripheral and central corneas, magnification 20x. (B) CNV area in the control group was increased from day 0 to 14; however, there was a mild decrease on day 14 post-alkali burn. Conversely, the catalpol-treated group exhibited a mild but significant decrease in CNV area on days 4, 7, 10 and day 14. *P<0.05 vs. PBS group. (C) Inflammatory index was reduced from day 0 to 14 in both groups. However, it was significantly lower in the catalpol-treated group on days 4, 7, 10 and 14. *P<0.05. CNV, corneal neovascularization.

by inducing apoptosis of underlying stromal cells, which promotes the infiltration of inflammatory cells that can cause further damage. To determine the effects of catalpol on alkali burn-induced apoptosis, a TUNEL assay was conducted. The majority of cells in the central corneas were TUNEL-positive on day 7 post-alkali burn in the PBS group. Conversely, the number of apoptotic cells was significantly reduced in the catalpol-treated corneas at day 7 compared with in the PBS group (Fig. 4A and B).

Catalpol alters the expression of VEGF and PEDF in alkali-burned rat corneas. CNV is controlled by the balance between pro- and antiangiogenic factors, including VEGF and PEDF. To investigate how catalpol prevents CNV in the alkali burn model, the present study analyzed the expression levels of VEGF and PEDF by western blotting and immunofluorescence (Fig. 5A). The results demonstrated that VEGF was expressed at low levels in normal rat corneas, and was markedly increased on day 14 post-alkali burn in the control group (data not shown). In the catalpol group, the expression of VEGF was much lower than in the control group on day 14. Conversely, PEDF was markedly decreased on day 14 post-alkali burn; however, PEDF was restored to some degree in the catalpol treatment group, although it was still somewhat lower than the expression in normal corneas (data not shown).

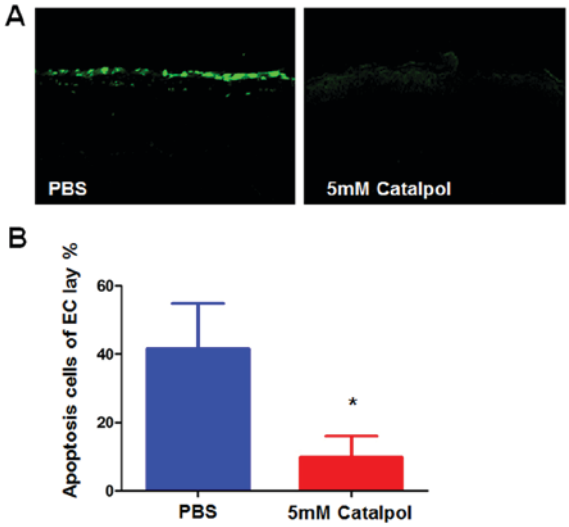

Figure 4. Catalpol reduces alkali burn-induced apoptosis of corneal cells, magnification, 40x. (A) TUNEL assay detected numerous apoptotic cells in the epithelia and endothelia in the PBS group on day 7. Conversely, in the catalpol-treated group markedly fewer apoptotic cells were detected. Fewer sporadic apoptotic cells were observed in the corneal endothelia at day 7. (B) Number of apoptotic cells was significantly reduced in the catalpol-treated group on day 7. *P<0.05.

Catalpol alters the expression of TNF-α and p-NF-κB p65 in alkali-burned rat corneas. The present study investigated the anti-inflammatory effects of catalpol post-alkali burn by measuring the expression levels of the inflammatory factors TNF-α and p-NF-κB p65 by western blotting (Fig. 6). On day 14 TNF-α expression was lower in the catalpol group vs. the PBS group (Fig. 6A and B). Furthermore, TNF-α was downregulated in catalpol group. Conversely, p-NF-κB p65 expression was increased in the catalpol-treated group (Fig. 6C and D). Catapol can inhibit inflammation induced by alkali-burn rat cornea.

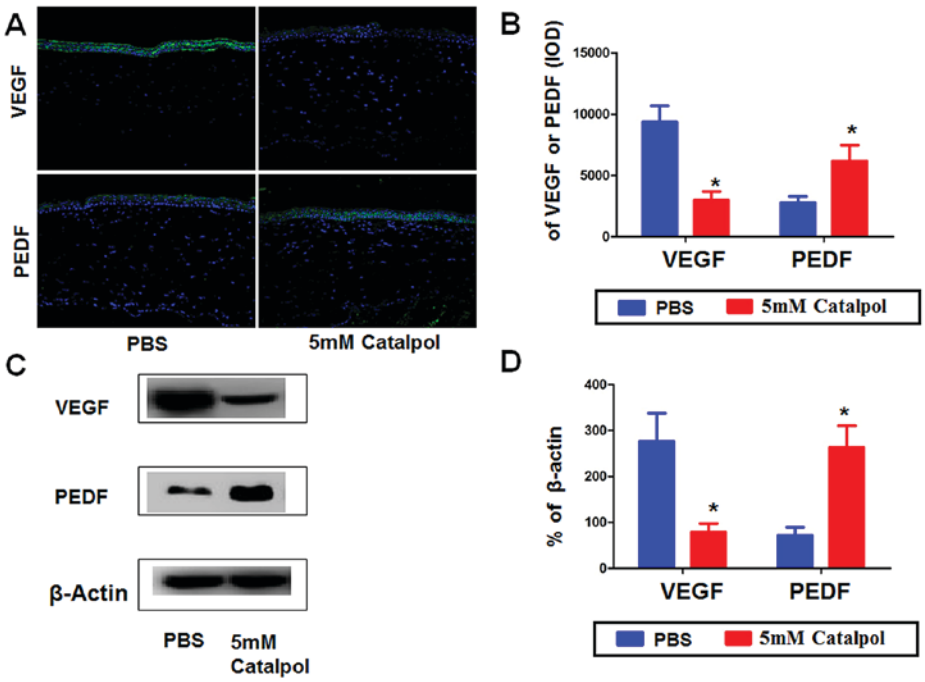

Figure 5. Effects of catalpol on VEGF and PEDF expression post-alkali burn. (A) Immunofluorescence determined VEGF and PEDF in control and Catalpol groups, magnification, 20x. (B) The integrated optical density analysis of VEGF and PEDF expression showed a significant difference between the two groups at day 14. (C) Western blotting demonstrated that VEGF expression was decreased and PEDF expression was increased in the catalpol-treated group compared with the control group at day 14. (D) Semi-quantification of protein expression detected to determine the significant differences in expression between the groups. *P<0.05. PEDF, pigment epithelium-derived factor; VEGF, vascular endothelial growth factor.

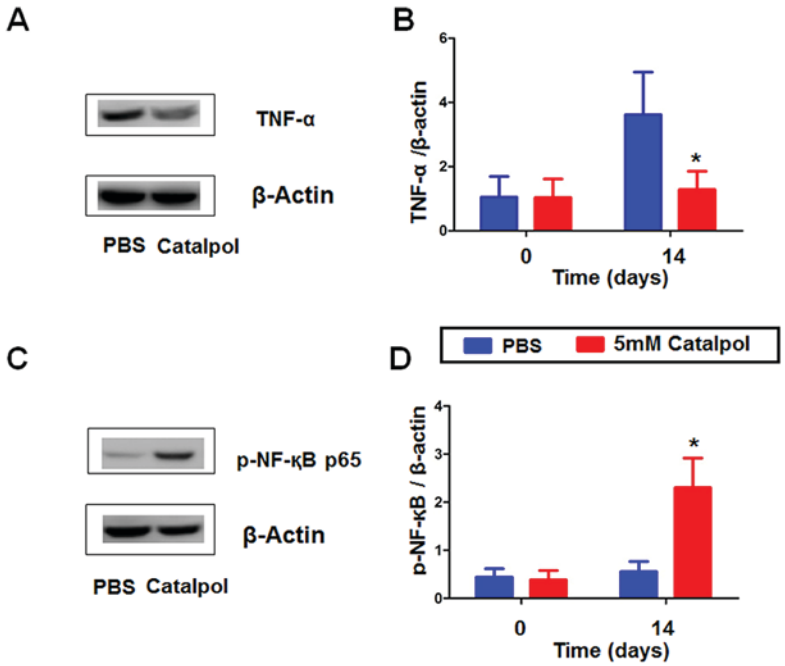

Figure 6. Effects of catalpol on TNF-α and p-NF-κB p65 expression post-corneal alkali burn. (A and B) Western blot analysis demonstrated that TNF-α in the control group was increased on day 14 post-alkali burn. In the catalpol-treated group, there was a marked downregulation of TNF-α on day 14. (C and D) p-NF-κB p65 was markedly increased on day 14 post-alkali burn in the catalpol-treated group. (B and D) Semi-quantification of protein expression determined the significant differences between the control and catalpol-treated groups with regards to TNF-α and p-NF-κB p65 expression on day 14. *P<0.05. p-NF-κB, phosphorylated-nuclear factor-κB; TNF-α, tumor necrosis factor-α.

Discussion

Corneal alkali burns result in the generation of progressive ocular disease, which aggravates inflammation and tissue injury, causing CNV-associated complications and ulceration. Although CNV is conducive to the elimination of pathogens

and tissue repair, it is also associated with reduced corneal transparency, thus resulting in damage to eye structure and visual function. In addition, CNV has been reported to be the main clinical cause of blindness (14). At present, the aim of future research is to develop novel, safe and effective anti-inflammatory and anti-angiogenic therapies for the treatment of CNV.

Catalpol has been reported to possess antioxidative, anti-inflammatory, anticancer, neuroprotective, diuretic, hypoglycemic, anti-hepatitis, hemostatic and antispasmodic properties (15,16). Ocular inflammatory factors and proapoptotic factors within ocular alkali-induced burns activate the apoptotic pathway, and simultaneously introduce a large number of polymorphonuclear and inflammatory cells to aggravate inflammation and injury. Choi *et al* (17) reported that catalpol alleviates the inflammatory response of THP-1 cells by inhibiting the activity of NF-κB. Basal expression of NF-κB has been reported in all cell types, and is known to serve a physiological role in the development of the cornea and normal physiological activities (16). Upon stimulation of the cornea by external factors, the NF-κB/inhibitory κB complex dissociates, and NF-κB is translocated into the nucleus where it binds to corresponding sites on target genes, thus activating gene transcription.

TNF-α is mainly produced by monocytes and macrophages, and can inhibit the activity of nitric oxide synthase, promote the expression of endothelial cell adhesion molecules, activate vascular endothelial cells, release platelet-derived growth factor and induce apoptosis of endothelial cells. Consequently, TNF-α can cause vascular proliferation and necrosis (17). Recently, it has been demonstrated that catalpol can reduce TNF-α and p-NF-κB expression (18). The results of the present study indicated that catalpol treatment reduced inflammation associated with alkali burns of the cornea and downregulated the expression of TNF-α and p-NF-κB.

VEGF is a specific marker protein of vascular endothelial cells, which is involved in the regulation of capillary vessel angiogenesis (19). VEGF can induce proliferation, response to chemokines and permeability of vascular endothelial cells, and participates in the formation of new blood vessels. In addition, VEGF can promote adhesion, migration and differentiation of mononuclear macrophages, and maintains these processes (20). Previously, it has been reported that that VEGF is an effective factor in the initiation and regulation of angiogenesis (21). PEDF is a specific anti-angiogenic factor and neurotrophic factor, which is expressed within the retinal pigment epithelium, iris and cornea (22). It has been reported that PEDF can promote endothelial cell apoptosis; however, it also inhibits migration of vascular endothelial cells and lumen formation (23). PEDF has a strong inhibitory effect on CNV and may be an important factor in controlling the progression of the disease (24). Evidence has demonstrated that the proangiogenic effects of catalpol may be associated with the upregulation of VEGF expression (25). Low doses of catalpol exert an inhibitory effect on the integrity of vascular endothelial cells. Studies have also reported that the protective effects of catalpol on vascular endothelial cells are dose-dependent. Low doses of catalpol exert an inhibitory effect on the integrity of vascular endothelial cells; however high doses of catalpol provide protective effects (26,27). In the present study, low concentrations of catalpol were administered as low doses of catalpol exert an inhibitory effect on the integrity of vascular endothelial cells; however high doses of catalpol provide protective effects. Western blotting revealed that catalpol can downregulate the expression levels of VEGF and upregulate the expression levels of PEDF to inhibit the formation of new blood vessels. In addition, catalpol was confirmed to inhibit the proliferation, invasion, migration and tube formation of HUVECs, which is associated with the inhibition of CNV (Fig. 1B).

As one of the main causes of blindness, CNV is also a risk factor for graft rejection following corneal allograft transplantation. Corneal alkali burns provide an integrated model of severe ocular surface disease, which results in corneal epithelial defects, keratitis, CNV and decreased corneal transparency (28,29). Such models are used to investigate the underlying mechanism and treatment of inflammation and angiogenesis due to ease of use and observation (30,31). The present study generated a corneal alkali-burned rat model, and the effects of the traditional Chinese medicine catalpol were determined. The results demonstrated that catalpol can inhibit the formation of CNV and the inflammatory response within alkali-burned rats, and confirmed that catalpol can inhibit HUVEC cell migration, tube formation, proliferation and apoptosis *in vitro*. Catalpol exhibits effects on corneal alkali burns via VEGF inhibition and PEDF upregulation. In addition, catalpol may reduce the expression of TNF and p-NF-kB-p65 to relieve the inflammatory response. Studies on the anti-inflammatory activity of catalpol further suggests that catalpol exerts therapeutic activity through attenuation of NF-κB activity (6,32). The present study provided a novel experimental basis for the treatment of CNV, as catalpol was demonstrated to inhibit the progression of CNV; however, the effects are dose dependent and further investigation into optimal dosage is required.

Acknowledgements

The present study was supported by grants from the National Natural Science Foundation of China (grant nos. 81300729, 81160118, 81460092 and 81660152), the Natural Science Foundation of Fujian Province (grant no. 2015J05170) and the ShanHai Foundation of China (grant no. 2013SH008).

References

1. Whitcher JP, Srinivasan M and Upadhyay MP: Corneal blindness: A global perspective. Bull World Health Organ 79: 214-221, 2001.
2. Hayashi K, Hooper LC, Detrick B and Hooks JJ: HSV immune complex (HSV-IgG: IC) and HSV-DNA elicit the production of angiogenic factor VEGF and MMP-9. Arch Virol 154: 219-226, 2009.
3. Zhang MC and Bian F: Emphasizing the prevention and anti-inflammation research of dry eye disease. Zhonghua Yan Ke Za Zhi 49: 6-7, 2013 (In Chinese).
4. Liu YR, Lei RY, Wang CE, Zhang BA, Lu H, Zhu HC and Zhang GB: Effects of catalpol on ATPase and amino acids in gerbils with cerebral ischemia/reperfusion injury. Neurol Sci 35: 1229-1233, 2014.
5. Wang JH, Zou L, Wan D, Zhu HF, Wang Y and Qin L: Review of Catalpol's pleiotropic signaling pathways. Zhong Guo Yao Li Xue Tong Bao Bian Ji Bu 9: 1189-1194, 2015 (In Chinese).
6. Bi J, Jiang B, Zorn A, Zhao RG, Liu P and An LJ: Catalpol inhibits LPS plus IFN-γ-induced inflammatory response in astrocytes primary cultures. Toxicol In Vitro 27: 543-550, 2013.
7. Wang Y, Zhang R, Xie J, Lu J and Yue Z: Analgesic activity of catalpol in rodent models of neuropathic pain, and its spinal mechanism. Cell Biochem Biophys 70: 1565-1571, 2014.

8. Han Y, Shao Y, Lin Z, Qu YL, Wang H, Zhou Y, Chen W, Chen Y, Chen WL, Hu FR, *et al*: Netrin-1 simultaneously suppresses corneal inflammation and neovascularization. Invest Ophthalmol Vis Sci 53: 1285-1295, 2012.
9. Policy statements adopted by the Governing Council of the American Public Health Association, November 15, 2000. Am J Public Health 91: 476-521, 2001.
10. Han Y, Shao Y, Liu T, Qu YL, Li W and Liu Z: Therapeutic effects of topical netrin-4 inhibits corneal neovascularization in alkali-burn rats. PLoS One 10: e0122951, 2015.
11. Yu Y, Zou J, Han Y, Quyang L, He H, Hu P, Shao Y and Tu P: Effects of intravitreal injection of netrin-1 in retinal neovascularization of streptozotocin-induced diabetic rats. Drug Des Devel Ther 9: 6363-6377, 2015.
12. Huang X, Han Y, Shao Y and Yi JL: Efficacy of the nucleotide-binding oligomerzation domain 1 inhibitor Nodinhibit-1 on corneal alkali burns in rats. Int J Ophthalmol 8: 860-865, 2015.
13. Arnaoutova I and Kleinman HK: In vitro angiogenesis: Endothelial cell tube formation on gelled basement membrane extract. Nat Protoc 5: 628-635, 2010.
14. Voiculescu OB, Voinea LM andAlexandrescu C: Corneal neovascularization and biological therapy. J Med Life 8: 444-448,2015.
15. Ismailoglu UB, Saracoglu I, Harput US and Sahin-Erdemli I: Effects of phenylpropanoid and iridoid glycosides on free radical-induced impairment of endothelium-dependent relaxation in rat aortic rings. J Ethnopharmacol 79: 193-197, 2002.
16. Li DQ, Zhou N, Zhang L, Ma P and Pflugfelder SC: Suppressive effects of azithromycin on zymosan-induced production of proinflammatory mediators by human corneal epithelial cells. Invest Ophthalmol Vis Sci 51: 5623-5629, 2010.
17. Choi HJ, Jang HJ, Chung TW, Jeong SI, Cha J, Choi JY, Han CW, Jang YS, Joo M, Jeong HS and Ha KT: Catalpol suppresses advanced glycation end-products-induced inflammatory responses through inhibition of reactive oxygen species in human monocytic THP-1 cells. Fitoterapia 86: 19-28, 2013.
18. Kleemann R, Zadelaar S and Kooistra T: Cytokines and atherosclerosis: A comprehensive review of studies in mice. Cardiovasc Res 79: 360-376, 2008.
19. Shao Y, Zhang Y, Yu Y, Xu TT, Wei R and Zhou Q: Impact of catalpol on retinal ganglion cells in diabetic retinopathy. Int J Clin Exp Med 9: 17274-17280, 2016.
20. Leung DW, Cachianes G, Kuang WJ, Goeddel DV and Ferrara N: Vascular endothelial growth factor is a secreted angiogenic mitogen. Science 246: 1306-1309, 1989.
21. Ferrara N and Davis-Smyth T: The biology of vascular endothelial growth factor. Endocr Rev 18: 4-25, 1997.
22. Phillips GD, Stone AM, Jones BD, Schultz JC, Whitehead RA and Knighton DR: Vascular endothelial growth factor (rhVEGF165) stimulates direct angiogenesis in the rabbit cornea. In Vivo 8: 961-965, 1994.
23. Liu JT, Chen YL, Chen WC, Chen HY, Lin YW, Wang SH, Man KM, Wan HM, Yin WH, Liu PL and Chen YH: Role of pigment epithelium-derived factor in stem/progenitor cell-associated neovascularization. J Biomed Biotechnol 2012: 871272, 2012.
24. Ortego J, Escribano J, Becerra SP and Coca-Prados M: Gene expression of the neurotrophic pigment epithelium-derived factor in the human ciliary epithelium. Synthesis and secretion into the aqueous humor. Invest Ophthalmol Vis Sci 37: 2759-2767, 1996.
25. Becerra SP: Focus on Molecules: Pigment epithelium-derived factor (PEDF). Exp Eye Res 82: 739-740, 2006.
26. Zhu HF, Wan D, Luo Y, Zhou JL, Chen L and Xu XY: Catalpol increases brain angio-genesis and up-regulates VEGF and EPO in the rat after permanent middle cerebral artery occlusion. Int J Biol Sci 6: 443-453, 2010.
27. Liu JY: Catalpol protect diabetic vascular endothelial function by inhibiting NADPH oxidase. Zhongguo Zhong Yao Za Zhi 39: 2936-2941, 2014 (In Chinese).
28. Liu X, Lin Z, Zhou T, Zong R, He H, Liu Z, Ma JX, Liu Z and Zhou Y: Anti-angiogenic and anti-inflammatory effects of SERPINA3K on corneal injury. PLoS One 6: e16712, 2011.
29. Saika S, Miyamoto T, Yamanaka O, Kato T, Ohnishi Y, Flanders KC, Ikeda K, Nakajima Y, Kao WW, Sato M, *et al*: Therapeutic effect of topical administration of SN50, an inhibitor of nuclear factor-kappaB, in treatment of corneal alkali burns in mice. Am J Pathol 166: 1393-1403, 2005.
30. Chen M, Matsuda H, Wang L, Watanabe T, Kimura MT, Igarashi J, Wang X, Sakimoto T, Fukuda N, Sawa M and Nagase H: Pretranscriptional regulation of Tgf-beta1 by PI polyamide prevents scarring and accelerates wound healing of the cornea after exposure to alkali. Mol Ther 18: 519-527, 2010.
31. Mochimaru H, Usui T, Yaguchi T, Nagahama Y, Hasegawa G, Usui Y, Shimmura S, Tsubota K, Amano S, Kawakami Y and Ishida S: Suppression of alkali burn-induced corneal neovascularization by dendritic cell vaccination targeting VEGF receptor 2. Invest Ophthalmol Vis Sci 49: 2172-2177, 2008.
32. Zhang A, Hao S, Bi J, Bao Y, Zhang X, An L and Jiang B: Effects of catalpol on mitochondrial function and working memory in mice after lipopolysaccharide-induced acute systemic inflammation. Exp Toxicol Pathol 61: 461-469, 2009.